Irreversible Alkylation of Human Serum Albumin by Zileuton Metabolite 2-Acetylbenzothiophene- S -oxide: A Potential Model for Hepatotoxicity

ARTICLE *in* CHEMICAL RESEARCH IN TOXICOLOGY · JANUARY 2008

Impact Factor: 3.53 · DOI: 10.1021/tx7001417 · Source: PubMed

4 AUTHORS, INCLUDING:

Fengping Li
University of Virginia
3 PUBLICATIONS **33** CITATIONS
SEE PROFILE

Mahendra Chordia
University of Virginia
76 PUBLICATIONS **958** CITATIONS
SEE PROFILE

Irreversible Alkylation of Human Serum Albumin by Zileuton Metabolite 2-Acetylbenzothiophene-*S*-oxide: A Potential Model for Hepatotoxicity

Fengping Li, Mahendra D. Chordia, Kellie A. Woodling, and Timothy L. Macdonald*

Department of Chemistry, University of Virginia, Charlottesville, Virginia 22901

Received April 27, 2007

2-Acetylbenzothiophene-*S*-oxide (2-ABT-*S*-oxide or **M1**) is a reactive metabolite of zileuton, a drug used in the treatment of asthma and is capable of conjugating with glutathione *in vitro*. Human serum albumin (HSA) is the most abundant protein in plasma and plays a critical role in detoxifying reactive oxygen species. The current research is focused on understanding the interaction between **M1** and HSA. The stability studies revealed the half-life of **M1** to be about 0.85 h in HSA, 1.82 h in human plasma, and 4.48 h in phosphate-buffered saline (PBS) as determined by first-order approximation. The alkylation rate constant k for HSA was 20 M^{-1} min^{-1}. After quenching with acetonitrile, the half-life of **M1** did not change significantly, indicating that **M1** is covalently bound to HSA. LC–MS and LC–MS/MS analysis of human plasma revealed the **M1** alkylated peptide ***P*** (m/z 870) formed by HSA conjugation and concomitant water elimination. The specific amino acid on HSA bound to **M1** was identified as Cys-34. This alkylation is observed to be concentration- and incubation-time-dependent in human plasma. HSA oxidized by *N*,*N*′-diacetyl-L-cystine exhibits a compromised ability of HSA to react with **M1**. The alkylated HSA diminished the binding affinity for warfarin. Furthermore, the alkylation was found to be irreversible in the dialysis experiment. In addition, **M1** decomposes to 2-ABT in the presence of HSA, presumably acting as an oxidant. The formation of 2-ABT in the incubation and the self-condensation of **M1** in PBS indicate that the alkylation of Cys-34 is only one of a number of reactions that occur in the presence of HSA. Irreversible protein modification may potentially lead to a loss of its function. HSA irreversible alkylation represents a model for other proteins to be potentially toxic and thus may help explain zileuton hepatotoxicity.

Introduction

Zileuton was first brought to the market in 1997 as a new type of drug for the treatment of asthma. As an inhibitor of 5-lipooxygenase, zileuton can inhibit the production of leukotriene-signaling molecules, effectively control asthma symptoms, and prevent its recurrence (*1*). However, after its release, elevated concentrations of alanine aminotransferase (ALT)[1] were observed in numerous patients and several cases of hepatotoxicity were recognized (*2*), prompting the removal of many patients from zileuton treatment.

Previous work from our laboratory demonstrated that 2-acetylbenzothiophene-*S*-oxide (2-ABT-*S*-oxide or **M1**) is a monooxidized reactive metabolite of zileuton. Cytochrome P450s 2E1 and 1A2 were shown to be two major enzymes responsible for oxidizing 2-acetylbenzothiophene (2-ABT) to **M1** (*3*). The covalent binding of drug-reactive metabolites to critical biomolecules, such as protein and DNA, is thought to be a significant cause of drug toxicity, and a number of studies have shown such covalent modification of biomacromolecules to result in mutation, cell necrosis, or apoptosis (*4*). The irreversible alkylation of **M1** to nucleophiles, such as glutathione (GSH) and *N*-acetylcysteine (NAc) (Scheme 1), was reported for the first time from this laboratory (*3*). However, the interaction between **M1** and other biological macromolecules, such as human proteins, remained unknown.

Scheme 1. Metabolism of Zileuton

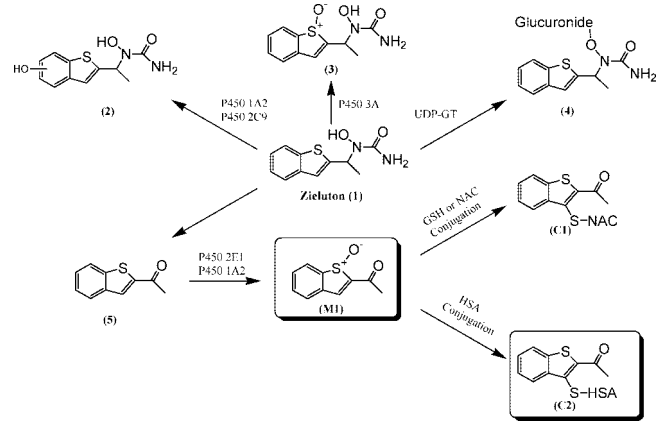

Human serum albumin (HSA), a protein of 585 amino acids, is synthesized in the liver as a preproalbumin and is secreted from the hepatocyte after a propeptide (RGVFRR) is cleaved (*5*). With a physiological concentration of ~600 μM (40 mg/mL), it is the most abundant protein in plasma and accounts for about 60% of the total proteins present in plasma samples. HSA plays an important role in the transportation and distribu-

* To whom correspondence should be addressed: Department of Chemistry, University of Virginia, McCormick Road, Charlottesville, VA 22901. Telephone: 434-924-7718. E-mail: tlm@virginia.edu.

[1] Abbreviations: **M1**, 2-acetylbenzothiophene-*S*-oxide; 2-ABT, 2-acetylbenzothiophene; HSA, human serum albumin; BSA, bovine serum albumin; GSH, glutathione; PBS, phosphate-buffered saline; IAA, iodoacetamide; DTT, dithiothreitol; Cys-34, cysteine 34; HPLC–MS, high-performance liquid chromatography–mass spectrometry; LC–MS/MS, liquid chromatography–tandem mass spectrometry; ALT, alanine aminotransferase; AcOH, acetic acid; NH_4OAc, ammonium acetate.

10.1021/tx7001417 CCC: $37.00
Published on Web 10/19/2007

tion of exogenous and endogenous ligands through the liver, intestine, kidney, and brain.

HSA contains two common binding sites, known as subdomains IIA and IIIA (*6*). These binding sites are very nonselective, and many drugs associate to either or both of these two subdomains. Cys-34 in HSA domain I accounts for about 80% of the total free thiols in plasma. The reduced cysteine residue also reacts with free radicals or inflammatory oxidants, and thus, HSA is an important component of the antioxidant defenses of the plasma or extracellular fluids. Cyanide ion (CN^-) reacts with disulfide bonds to form thiocyanate derivatives and has been shown to form a covalent adduct with Cys-34 on HSA in human plasma (*7*). The covalent binding of several drugs with HSA or BSA through Cys-34 has also been identified (*8, 9*). For example, acetaminophen has been demonstrated to interact with Cys-34 in BSA (*8*). Gold-based antiarthritic drugs ($AuPEt_3Cl$, $Na_3[Au(S_2O_3)_2$, and $Na[Au(CN)_2]$) also bind to HSA at Cys-34 (*9*). The ability of HSA to bind to many drugs covalently, as well as noncovaletly, is significantly compromised when Cys-34 is oxidized to form a disulfide (*10*). Because the covalent binding of reactive metabolites with proteins *in vivo* plays a critical role leading to toxicity, we chose HSA as a protein model to study the reactivity of **M1** with proteins *in vitro*. In addition, alkylated HSA may serve as a marker of reactive intermediate generation and potential for toxicity.

In the present work, we sought to probe the interaction between the zileuton-reactive metabolite **M1** and HSA and correlate the reactivity of HSA to that of GSH and NAc as reported earlier. The detailed investigations led us to discover that HSA indeed gets alkylated by **M1** at Cys-34. The relevance of alkylation of HSA with **M1** to potential hepatotoxicity is discussed.

Experimental Procedures

Chemicals and Instruments. Fatty-acid- and globulin-free HSA and human plasma were purchased from Sigma (St. Louis, MO). Sequencing-grade modified trypsin was procured from Promega. All other chemicals used were of the highest quality available and purchased from Sigma-Aldrich. Nanopure water (MilliQ) was used to prepare all solutions. The Waters 600E HPLC system was equipped with a Waters 468 tunable absorbance detector. high-performance liquid chromatography–mass spectrometry (HPLC–MS) was performed on Thermo-Finnigan LCQ classic ion-trap mass spectrometer with electrospray ionization (ESI). Data were processed using the Xcalibur version 1.1 software.

Synthesis of 2-ABT-*S*-oxide. 2-ABT-*S*-oxide synthesis was reported previously (*3*).

Synthesis of Oxidized HSA. Oxidized HSA was prepared by a modified procedure as reported in the literature (*10*). A total of 50-fold (3 mM) *N*,*N*′-diacetyl-L-cystine $(Ac\text{-}Cys\text{-}OH)_2$ was incubated at 37 °C with 4 mg/mL HSA for 2, 8, 12, 24, and 48 h. The excess *N*,*N*′-diacetyl-L-cystine and L-cysteine were removed at each time point by a Microcon YM-10 filter and washed by phosphate-buffered saline (PBS) 3 times. The oxidized protein was collected for later experiments.

Stability of M1 in HSA. HSA (40 mg/mL) or human plasma was incubated with 100 μM **M1** in 100 mM PBS at 37 °C. The total volume was 100 μL. After each incubation (0, 20, 40, 60, 80, or 100 min), 100 μL of 2% acetic acid was added to the solution. High-molecular-weight protein was removed using a Microcon YM-10 filter (Millipore) by centrifuging at 14 000 rpm at 4 °C. The filtrate containing unreacted **M1** was injected into HPLC–UV and detected at the wavelength of 253 nm. Samples were separated by a Waters Delta Pak C_{18} (3.9 × 150 mm) column. The amount of **M1** was measured by comparing it to 50 μM zileuton as the internal standard (zileuton was added at the end, just before measurements). The gradient conditions used for analysis were 65:35 H_2O [0.02% trifluoroacetic acid (TFA)]/methanol, where the methanol percentage was increased to 100% over 25 min. The half-life ($t_{1/2}$) of **M1** was measured by a first-order approximation (*11*). When ln[**M1**] was plotted versus time, the slope of a curve ($-k_{obs}$) can be calculated. The $t_{1/2}$ is equal to ln $2/k_{obs}$. Each experiment was repeated at least 3 times.

To measure the half-life of **M1** in oxidized HSA, slightly modified procedure was used. Because 40 mg/mL HSA turned to gel after 48 h of oxidation with *N*,*N*′-diacetyl-L-cystine, 8 mg/mL HSA was used instead and a relative concentration of HSA to that of **M1** was kept constant to obtain a close comparison (6:1). Zileuton (15 μM) was used as the internal standard. **M1** (20 μM) and 48 h oxidized HSA (8 mg/mL, 120 μM) were incubated. The half-life was measured as described above.

Acetonitrile can denature HSA and perturbs the hydrophobic nonbonding interaction between **M1** and HSA. To determine if the interaction between **M1** and HSA is covalent or noncovalent, 90 μL of acetonitrile and 10 μL of 20% acetic acid were used to quench the conjugation reaction after each time point, as mentioned above. After centrifugation at 14 000 rpm for 15 min at 4 °C, the supernatant was analyzed by HPLC–UV.

To determine the alkylation rate constant k for the consumption of **M1** by HSA, another series of incubations with varying HSA concentrations (0, 10, 20, 40, or 60 mg/mL) were performed using the conditions outlined above. The alkylation rate constant k was measured from the slope of the curve of k_{obs} versus the HSA concentration (*11*).

Determination of the Alkylation Domain(s) on HSA by M1. Warfarin and/or ibuprofen (600 μM) were added to 40 mg/mL HSA in 100 mM PBS buffer. The solution was incubated at 37 °C for 40 min before 100 μM **M1** was added, and the half-life of **M1** was measured, as mentioned above.

Alkylation of HSA/Plasma. M1 (300 μM) was incubated with HSA/plasma (4 mg/mL) in 500 μL of 0.25 M Tris-HCl buffer (pH 7.4). After 1 h, low-molecular-weight entities were removed by centrifugation through a Microcon YM-10 filter. The remaining protein was washed thoroughly (200 μL × 3) with 0.25 M Tris-HCl buffer and centrifuged to remove excess **M1**. HSA/plasma was reconstituted in 500 μL of Tris-HCl buffer with 6 M guanidine–HCl and 53 mM dithiothreitol (DTT) and incubated at 55 °C for 1 h. After the solution was cooled to room temperature, excess iodoacetamide (150 mM, ~3 times of DTT) in 0.25 M Tris-HCl buffer was added and the solution was incubated in the dark at room temperature for 30 min. The protein was then desalted by a PD-10 column (GE Healthcare) and detected by the Biorad assay. Ammonium bicarbonate (0.4%, w/w) was used to equilibrate the column prior to use and to elute the protein. Fractions containing the protein were collected (total volume ~ 2 mL).

Tryptic Digestion of HSA. The desalted HSA (700 μL) obtained above was digested by trypsin (20 μg, Promega) (50:1, w/w) overnight at 37 °C. The digestion was quenched by the addition of 20% acetic acid. Before MS analysis, samples were diluted (1:3) with 5% acetic acid and 15 μL of the diluted solutions was injected onto a Jupiter C_{18} reversed-phase column (2.0 × 150 mm) by liquid chromatography (LC) equipped with an auto-sampler. Separation was performed with a three-step gradient with acetonitrile (solvent A) and 0.1% formic acid (solvent B). The gradient conditions were as follows: 100% solvent B decreasing to 68% for 85 min and to 45% for 40 min.

Liquid Chromatography–Mass Spectrometry (LC–MS) of Peptides. Characteristic peptides from HSA tryptic digest modified by iodoacetamide (http://us.expasy.org/proteomics) were first confirmed according to their m/z ratios from the LC–MS spectrum. The alkylated peptide(s) was then identified manually by searching for a new additional peak when compared to a control experiment. The ESI ion source was operated in positive-ion mode. A full scan was performed from m/z 235–2000. Parameters for ESI–MS were set as follows: heated capillary temperature of 190 °C, spray voltage of 4.0 kV, capillary voltage of 3.0 V, sheath gas flow rate at 70 units, and auxiliary gas flow rate at 20 units.

Tandem Mass Spectrometry (MS/MS) Experiments. The parent ion was set at *m/z* 831 for iodoacetamide (IAA) alkylated peptide ***Q*** or at *m/z* 870 for **M1** alkylated peptide ***P***. The collision energy was set at 30%, with an isolation width of 3 Da.

Confirmation of the Alkylation Reaction. The trypsin-digested HSA solution as described above was divided equally (700 μL each) into two eppendorfs. In one tube, 300 μL of 20% AcOH was added and the sample was analyzed under conditions "a" (positive-ion mode HPLC–MS, 0.1% formic acid, pH 2) and "b" (negative-ion mode LC–MS, 10 mM NH_4OAc, pH 6). The second tube was treated with 300 μL of 10 mM NH_4OAc, and the sample was assayed under conditions "c" (positive-ion mode HPLC–MS, 0.1% formic acid, pH 2) and "d" (negative-ion mode LC–MS, 10 mM NH_4OAc, pH 6). From all assays, the alkylated peptide ***P*** was identified when compared to the control experiment (no **M1**). The parameters for ESI–MS negative-ion mode were almost the same as those of the positive-ion mode, except the conditions: spray voltage of 4.5 kV and capillary voltage of −37 V.

Concentration- and Time-Dependent M1 Conjugation with HSA in Human Plasma. Several assigned concentrations of **M1** (3, 10, 25, 50, 100, and 300 μM) were each incubated with 4 mg/mL plasma for 1 h. The alkylated proteins were processed and digested as described above. The peak areas of the alkylated peptide ***P*** with *m/z* 870 were recorded as functions of **M1** concentrations. Each data point was repeated at least twice.

In another experiment, **M1** (100 μM) was incubated with 4 mg/mL plasma for different times (0, 1, 4, 12, 24, and 48 h). Proteins were processed and digested as described above. Only the peak areas of the alkylated peptide ***P*** with *m/z* 870 were recorded as functions of the incubation times. Each data point was repeated at least twice.

Effect of Denatured HSA on M1 Alkylation. HSA (4 mg/mL) was denatured by 6 M guanidine for 18 h. The denatured HSA was incubated with **M1** (300 μM) for 1 h. The alkylation percentage was calculated by dividing the peak area of the peptide ***P*** over the sum of the peak areas of peptides ***P***, ***Q***, and ***R***, and the data were compared to the native HSA.

Incubation of M1 with Oxidized HSA. HSA (4 mg/mL) was oxidized by 3 mM *N*,*N*′-diacetyl-L-cystine for 2, 8, 12, 24, and 48 h. The protein was then desalted by a Microcon YM-10 filter and washed with 0.25 M Tris-HCl (200 μL × 3). **M1** (100 μM) was incubated with each oxidized HSA sample for 2 h. The digestion and LC–MS analysis were performed as described above.

Effect of HSA Alkylation by M1 on Warfarin Binding. HSA (4 mg/mL) was incubated with 300 μM **M1** for 36 h. The sample was filtered through a Microcon YM-10 filter, and the residue was used further to incubate with warfarin for 30 min. At the end of incubation, the solution was filtered again by a Microcon YM-10 filter and the filtrate was analyzed by HPLC–MS.

Dialysis of Alkylated Human Plasma. M1 (100 μM) was incubated with 4 mg/mL plasma for 1 h. The sample was then dialyzed against PBS buffer for 3 days using a 0.1–0.5 mL 10000 molecular weight cut-off (MWCO) Slide-A-Lyzer dialysis cassette (Pierce, Rockford, IL) at 4 °C. The PBS buffer was changed everyday. After the dialysis, the solution was digested and analyzed, as mentioned above. The peak area of the alkylated peptide was compared to the one without dialysis. The experiment was repeated twice.

Results

Stability Study. In the kinetic study, the half-life of **M1** in HSA and the alkylation rate constant *k* of HSA were determined. Because the concentration of HSA (600 μM) is 6 times higher than **M1** (100 μM), the half-life ($t_{1/2}$) of **M1** is measured by a first-order approximation (*11*). When ln[**M1**] is plotted versus time to calculate the slope of a curve ($-k_{obs}$), the $t_{1/2}$ is equal to $0.6932/k_{obs}$. The half-life of **M1** is 0.85 ± 0.12 h in 40 mg/mL HSA (Table 1). This is approximately 5-fold less than in the phosphate buffer solution (4.48 ± 0.56 h) and about 4.5-fold less than in a 600 μM GSH solution (3.83 ± 0.25 h). With 48 h oxidized HSA, the half-life of **M1** is 4.14 ± 0.29 h.

Table 1. Half-Life of M1 under Various Conditions

condition[a]	$t_{1/2}$ (h)
control	4.48 ± 0.56
GSH[b]	3.83 ± 0.25
HSA	0.85 ± 0.12
plasma	1.82 ± 0.23
oxidized HSA[c]	4.14 ± 0.29
HSA plus ibuprofen	1.23 ± 0.34
HSA plus warfarin	1.16 ± 0.38
HSA plus ibuprofen and warfarin	1.08 ± 0.25

[a] All incubations in 100 mM potassium phosphate buffer at pH 7.4. [b] Concentrations of GSH, proteins, ibuprofen, and warfarin were 600 μM. [c] The concentration of 48 h oxidized HSA was 120 μM.

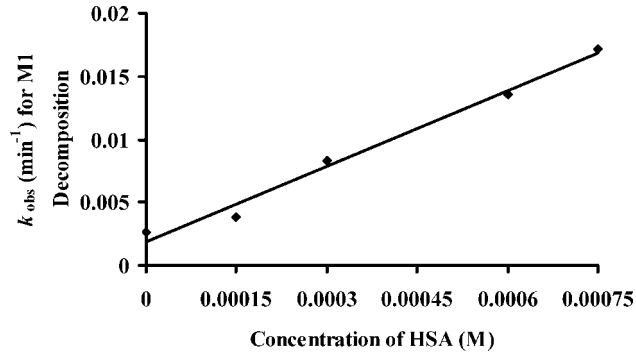

Figure 1. Effect of the HSA concentration on the decomposition of **M1**.

Acetonitrile quench was used to determine the nature of the interaction between **M1** and HSA. The half-life of **M1** was 0.98 ± 0.15 h, close to the half-life observed without acetonitrile.

The alkylation rate constant *k* for the consumption of **M1** by HSA was measured from the slope of the curve of k_{obs} versus the HSA concentration (Figure 1). The value of *k* for HSA was 20 M^{-1} min^{-1}. The *y* intercept is the rate constant for the phosphate buffer solution, which was 0.0019 M^{-1} min^{-1}, about 10^4 times less than in HSA solution.

Warfarin and Ibuprofen Competition Analysis. Warfarin binds strongly to HSA subdomain IIA (Sudlow's drug site I), with the binding constant of 3.3×10^5 M^{-1} (*12*). The binding constant of ibuprofen to HSA subdomain IIIA (Sudlow's drug site II) is 2.7×10^6 M^{-1} (*13*). The half-life of **M1** in HSA was 1.16 ± 0.38 h in the presence of warfarin, 1.23 ± 0.34 h in the presence of ibuprofen, and 1.08 ± 0.25 h in the presence of both warfarin and ibuprofen. The data are represented in Table 1.

Identification of an Alkylated Peptide by M1 on HSA. Peptides from the **M1** and HSA incubation were compared to the control experiment (without **M1**) to identify any new peak(s). From the incubation of **M1** with HSA, only one additional peptide was observed at 107 min with *m/z* 870 (peptide ***P***) (along with peaks at 95.64 and 92.36 min as in the control experiment) from the LC–MS chromatogram by manually searching peaks (Figure 2A). An identical alkylated peak was observed when similar experiments were performed with human plasma (Figure 2B). In control experiments, wherein only IAA was used (Figure 2C), a peak with the retention time at 95.64 min (peptide ***Q***) was observed. This corresponded to a peptide with *m/z* 831. In addition, another peak at the retention time of 92.36 min with *m/z* 812 (peptide ***R***, Figure 2D) was identified. A search for peptide ***P*** (*m/z* 870) in the control experiment of HSA without **M1** revealed the absence of any such peak, as exhibited in

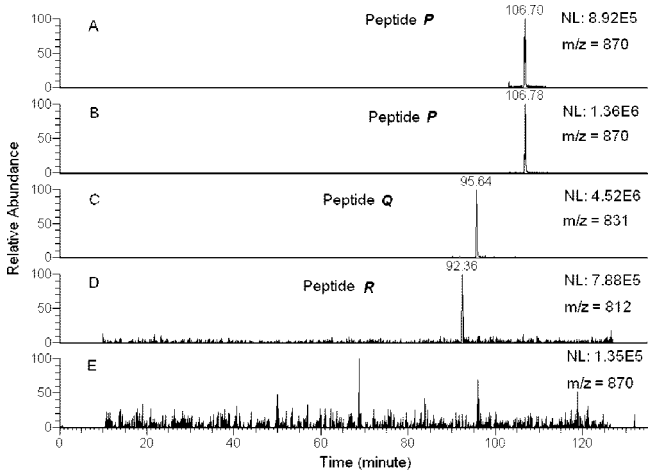

Figure 2. HPLC–MS chromatograms of peptides from various experiments. (A) **M1** and HSA incubation, (B) **M1** and human plasma incubation, (C) IAA with HSA (control), (D) the unmodified peptide from HSA (negative control), and (E) a search for the peak at *m/z* 870 (peptide ***P***) in the control.

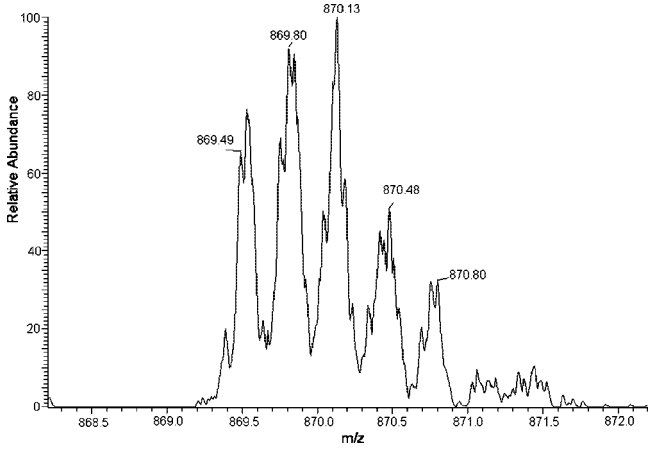

Figure 3. ZoomScan mass spectrum of the peptide ***P*** (*m/z* 870) at 107 min.

Figure 2E. The amino acid sequence for these peptides is assigned as Ala-21 to Lys-41 (ALVLIAFAQYLQQCPFEDHVK).

Determination of the Conjugated Peptide Charge State. The charge state and corresponding molecular weight of the selected peptide was determined by ZoomScan analysis. The *m/z* difference between two adjacent peaks was 0.33 Da (Figure 3), which concludes that the charge state of the adducted peptide was +3.

Liquid Chromatography–Tandem Mass Spectrometry (LC–MS/MS) of the Conjugation Peptide. LC–MS/MS was performed on the peptide ***P*** with **M1** modification. Relevant b and y ions were identified (Figure 4A). In the b series, fragments b_3^+ (*m/z* 283.7), b_4^+ (*m/z* 397.0), b_6^+ (*m/z* 581.1), b_8^+ (*m/z* 799.3), b_{11}^+ (*m/z* 1203.4), b_{12}^+ (*m/z* 1331.7), and b_{13}^+ (*m/z* 1460.6) were from the original peptide. In the y series, natural y_4^+ (*m/z* 498.0) and y_5^+ (*m/z* 627.3) were found. Furthermore, in the y series, fragment ions y_{12}^+ (*m/z* 1681.5), y_{12}^{2+} (*m/z* 841.0), y_{13}^{2+} (*m/z* 904.9), y_{14}^{2+} (*m/z* 940.5), y_{15}^{2+} (*m/z* 1014.0), y_{16}^{2+} (*m/z* 1049.6), y_{17}^{2+} (*m/z* 1106.0), y_{18}^{2+} (*m/z* 1162.7), and y_{19}^{2+} (*m/z* 1212.2) were identified as alkylated ions with the mass addition of 174 Da when compared to the control experiment.

Peptide ***Q***, with *m/z* 831, is modified by IAA. Figure 4B is the MS/MS spectrum. Similar to the Figure 4A, fragment ions b_3^+ (*m/z* 283.8), b_4^+ (*m/z* 396.9), b_5^+ (*m/z* 510.0), b_6^+ (*m/z* 581.1), b_{11}^+ (*m/z* 1203.5), b_{12}^+ (*m/z* 1332.2), and b_{13}^+ (*m/z* 1459.6) were the same as the original amino acids. In the y series, the *m/z* ratios of y_4^+ (*m/z* 498.1) and y_5^+ (*m/z* 627.0) did not change. However, y_{12}^{2+} (*m/z* 782.6), y_{13}^{2+} (*m/z* 846.5), y_{14}^{2+} (*m/z* 882.1), y_{15}^{2+} (*m/z* 955.5), y_{16}^{2+} (*m/z* 991.1), y_{17}^{2+} (*m/z* 1047.6), y_{18}^{2+} (*m/z* 1104.3), and y_{19}^{2+} (*m/z* 1153.7) all had a mass increase of 58 Da (molecular weight of IAA) when compared to the amino acid sequence in the negative control.

Confirmation of the Alkylation Reaction. Under "a" and "c" conditions (positive-ion mode as described in the Experimental Procedures), an alkylated peptide with *m/z* 870 was identified at 107 min. Under "b" and "d" conditions (negative-ion mode as described in the Experimental Procedures), an alkylated peptide with *m/z* 1302.5 was identified at 107.8 min. This peptide in the LC–MS negative-ion mode is the same one as in the LC–MS positive-ion mode but with two negative charges (Scheme 2).

Concentration- and Time-Dependent M1 Conjugation with HSA in Human Plasma. The conjugation behavior of **M1** to HSA in human plasma was measured at different incubation times and **M1** concentrations using semiquantitation. The concentration of HSA in 4 mg/mL plasma was ~30 μM. From low to high concentrations (3–300 μM) of **M1**, the increased intensity of the same alkylated peak was observed (Figure 5). From 3 to 300 μM of **M1**, the peak area of the alkylated peptide increased by ~7-fold.

For varied incubation times, the same alkylated peak was measured by plotting the peak areas versus the incubation times. The amount of **M1** (100 μM) was about 3 times that of HSA (~30 μM) in plasma. The peak areas of the alkylated peptide are linearly proportional to the incubation times as shown in Figure 6. From the incubation time of 0 min to 48 h, the peak area was increased by about 25-fold.

Effect of Denatured HSA on M1 Alkylation. From the incubation of 30 μM HSA and 300 μM **M1**, the maximum alkylation percentage obtained was 8.5%, which is ~28-fold more than that of the denatured HSA (0.3%).

Alkylation of M1 with Oxidized HSA. HSA was oxidized with *N*,*N*′-diacetyl-L-cystine at various time points. With the increased formation of oxidized HSA, the amount of the peptide ***P*** formation is reduced (Figure 7). The percentage of the alkylation change is 52% between 2 and 48 h of oxidation.

Effect of M1 Alkylated HSA to Warfarin Binding. The binding affinity of warfarin to native and **M1**-alkylated HSA was determined by the ratio of the amount of unbound warfarin over the internal standard (oxidized gluthione, GSSG). For the alkylated HSA, the unbound warfarin was ~45% more than that of the nonalkylated HSA (Figure 8), indicating a diminished binding affinity for warfarin.

Dialysis. After 3 days of dialysis in PBS solution, the peak area of the alkylated peptide was 134 ± 10% of the area without dialysis. It appears that alkylation was still proceeding in the dialysis experiment. Overall, from the dialysis experiment, the alkylation of HSA in plasma by **M1** is found to be irreversible.

Discussion

HSA is the principal protein in plasma, constituting ~60% of the total proteins. It binds and transports a large number of endogenous and foreign molecules throughout the body and detoxifies many reactive species. Our studies have used HSA as a model for the interaction of **M1** with proteins, but the potential *in vivo* formation of **M1**–HSA adducts could have

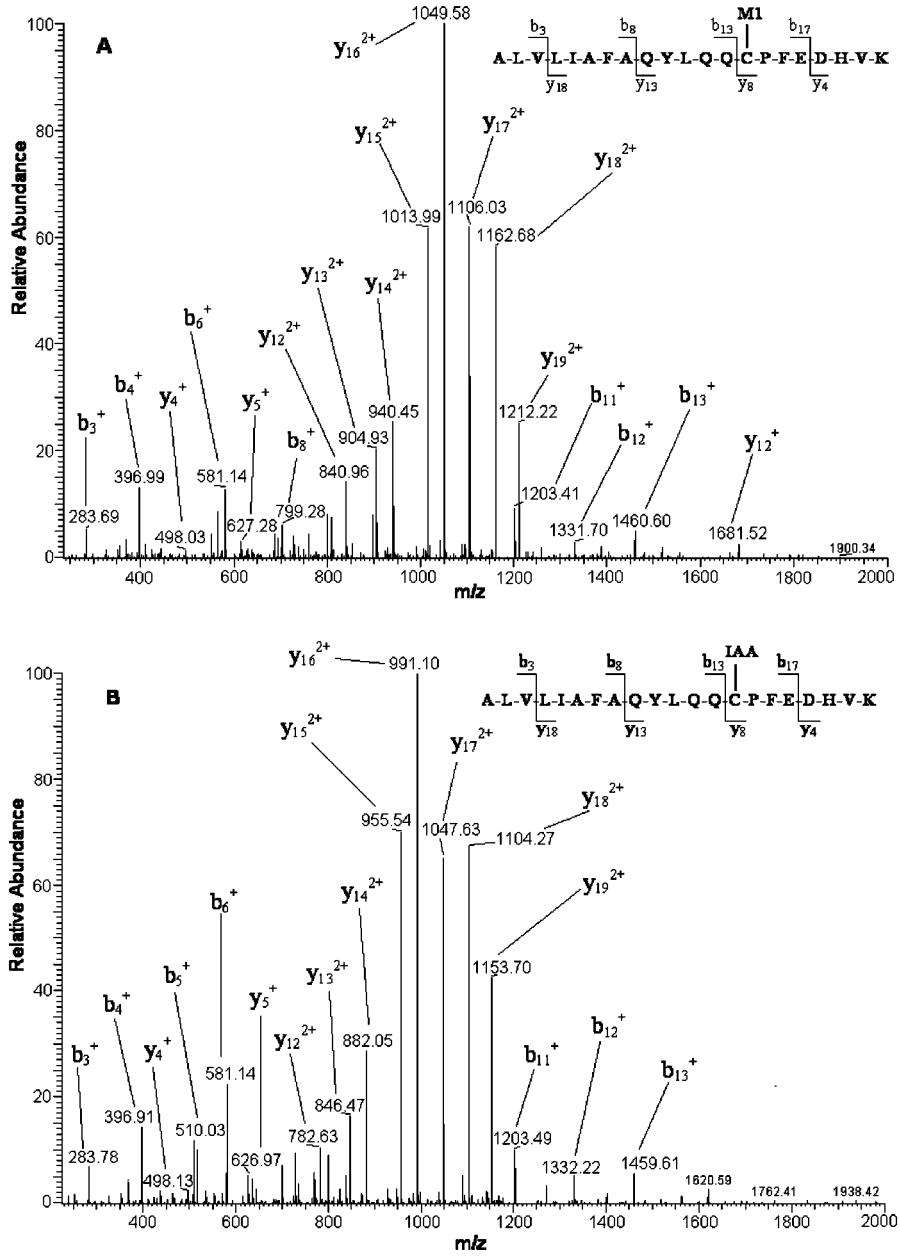

Figure 4. LC–MS/MS spectra of (A) the peptide ***P*** (*m*/*z* 870) from **M1** and HSA conjugation and (B) the peptide ***Q*** (*m*/*z* 831) from IAA and HSA conjugation.

Scheme 2. Methods Used To Identify the Alkylated Peptide under Various Conditions by HPLC–MS Positive- and Negative-Ion Modes

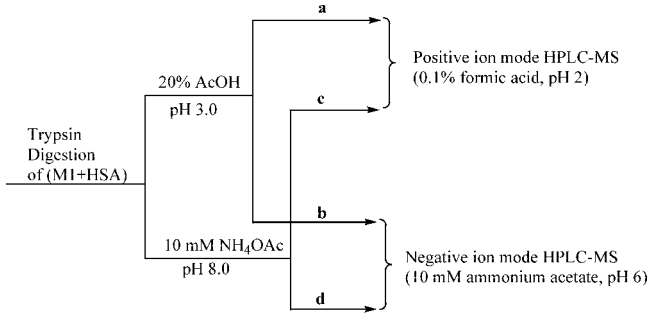

additional implications for toxicity or as a marker for the production of reactive intermediates.

From the kinetic study, the half-life of **M1** (0.85 ± 0.12 h) in HSA is about 5-fold less than in PBS (4.48 ± 0.56 h). This

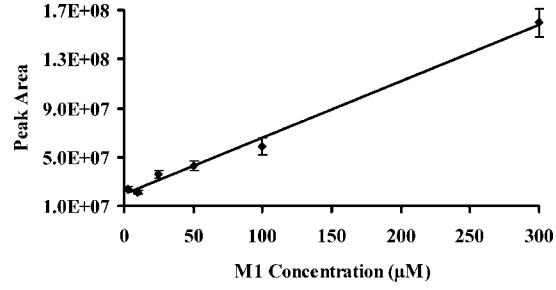

Figure 5. Concentration-dependent alkylation of HSA by **M1** in plasma solution.

suggests that HSA enhances the decomposition of **M1** through either covalent binding or the catalysis of alternate decomposition pathways. The fact that significant noncovalent association of **M1** with HSA did not affect the observed half-life was demonstrated by HSA denaturation (**M1** half-life = 0.98 ± 0.05 h) versus a nondenatured control (**M1** half-life = 0.85 ±

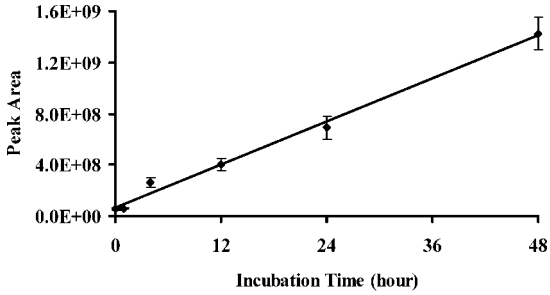

Figure 6. Time-dependent alkylation of HSA by **M1** in plasma solution.

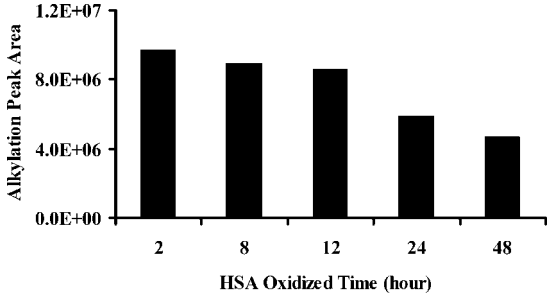

Figure 7. Effect of oxidized HSA on the conjugation with **M1** (100 μM).

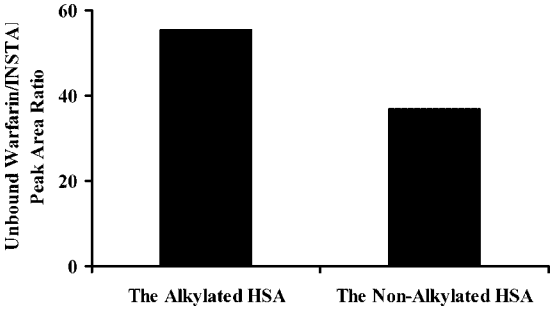

Figure 8. Effect of **M1**-alkylated HSA on warfarin binding over 30 min of incubation.

0.12 h). Subsequent mass spectrometric analysis confirmed that the interaction between HSA and **M1** is covalent, and the alkylation rate constant (k) of HSA for **M1** was found to be 20 M^{-1} min^{-1}. It is 0.66 times larger than that for the decomposition of an oxazinane metabolite of felbamate (12.04 M^{-1} min^{-1}) (*14*) and 14 times lower than that for the degradation of 4-hydroxycyclophosphamide (285 M^{-1} min^{-1}) (*11*).

The half-life of **M1** in HSA (600 μM) is about 4.5 times lower than that in GSH (600 μM), even though both of the alkylation reactions occur at a free sulfhydryl group. These data suggest that the protein "pocket" of HSA either facilitates the alkylation reaction of the thiol with **M1** or inhibits the reversal of the initial **M1**–thiol adduct. This was further supported by the observation that denatured HSA has much lower **M1** alkylation (0.3%) to that with native HSA (8.5%). Certainly, *retro*-alkylation or thiol elimination reactions of a number of adducts of thiols with electrophiles have been observed.

The maximum alkylation of HSA by **M1** under the conditions studied was found to be about 8.5%. However, the formation of alkylated peptide ***P*** appears quantitatively less efficient. Further investigation into the fate of **M1** during the incubation with HSA revealed two significant additional reaction pathways: (a) **M1** undergoes self-condensation to form a dimeric compound, a dimer with the loss of a water molecule, and oligomers; and (b) **M1** can act as an oxidant, undergoing reduction to 2-ABT and presumably causing the oxidation of HSA or other thiols (data presented in the Supporting Information). These observations help to explain the complexity of **M1** decomposition and the lack of stoichiometric formation of alkylated peptide ***P*** with the loss of **M1**. HSA is susceptible to oxidation by *tert*-butyl hydroperoxide (*t*-BuOOH) to form an oxidized dimer (*19*). It is interesting to note here that the oxidation of HSA to its dimer by **M1** should lead to the formation of more IAA alkylated peptide ***Q*** after DTT reduction. Indeed, ~75% of peptide ***Q*** was identified in the same experiment.

To identify the HSA binding domain with which **M1** interacts, a series of competition experiments were performed with warfarin and ibuprofen. Warfarin and ibuprofen exhibit well-established binding primarily to HSA subdomains IIA and IIIA, respectively (*12, 13*). Our studies find that these compounds do not have a profound effect on **M1** binding and imply that HSA subdomains IIA and IIIA are not involved in **M1** decomposition (Table 1).

In attempts directed at pinpointing the exact amino acid(s) of HSA with which **M1** interacts, detailed LC–MS studies were performed. The alkylation of HSA at Cys-34, Lys-190, Lys-199, His-242, His-247, and Tyr-411 by a variety of exogenous species have been reported (*8, 9, 14–17*). The LC–MS analysis of tryptic digests of HSA from control experiments indicated a peak at 95.6 min with m/z 831, while that from **M1**-treated HSA gave a peak at 107 min with m/z 870. MS/MS analysis of these fragments (b and y ions, Figure 4) confirmed that both contain the same amino acid sequence (ALVLIAFAQYLQQCPFEDH-VK). The peptide fragment obtained in the control experiment (no **M1**) exhibited a m/z increase of 19 (alkylation by IAA, mass increase of 57), while the same peptide obtained from the **M1** incubation experiment exhibited a m/z increase of 58 (conjugation with **M1** followed by water elimination, mass increase of 174), suggesting that these peptide fragments have a +3 charge. This was further confirmed by ZoomScan analysis (Figure 3). The detailed LC–MS/MS analysis (Figure 4A) of the alkylated peptide ***P*** revealed that one of three amino acids from Cys-34, Pro-35, and Phe-36 may be modified by **M1**. However, Cys-34 is the only nucleophilic amino acid present in the tripeptide sequence capable of alkylation. The reactivity of Cys-34 is comparable to that of GSH studies reported earlier from this laboratory (*3*). The loss of a water molecule from the **M1** alkylated peptide ***P***, although not surprising, is the only exclusive peptide fragment observed from the incubation.

The alkylation of GSH with **M1** without the loss of water is observed independently in the previous studies (*3*). It was also demonstrated that an acidic medium promotes water elimination from the mercaptoethanol adduct as reported by Mansuy et al. in their *S*-oxide adducts (*18*). To observe the direct adduct between HSA and **M1** without the loss of water, a few control experiments were performed, as shown in Scheme 2. However, under mild pH and negative-ion mode HPLC–MS conditions, only water eliminated conjugated peptide ***P*** and none of the direct alkylated product was observed. It is possible that the alkylation and subsequent dehydration are catalyzed by HSA itself.

It is very interesting to note that the felbamate metabolite, 2-phenylpropenal, interacts with HSA in reversible covalent fashion at subdomain IIA with His-242/247 (*14*). In contrast, zileuton metabolite **M1** irreversibly conjugates with Cys-34 at subdomain IA on HSA and forms a mono-alkylated peptide (Scheme 3). The two reactive metabolites of these two drugs conjugate with separate amino acids (Cys-34 and His-242/247) because of their binding specificity, imparted by their structures,

Scheme 3. Proposed Mechanism of M1 and HSA Conjugation

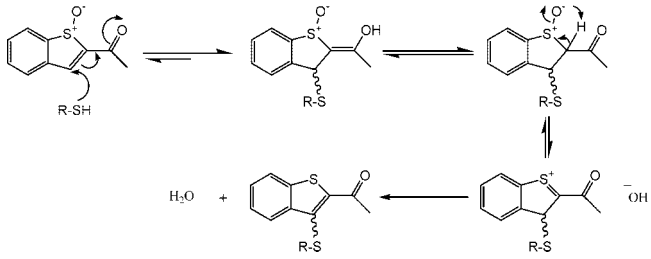

and the microenvironment present on the protein, suggesting the availability of multiple pathways.

M1 readily reacts with HSA to afford an alkylated peptide *in vitro*. To mimic a realistic biological environment, human plasma was used to determine whether **M1** conjugation remains a signficant pathway for **M1** consumption *ex vivo*. Indeed, the same alkylated peptide ***P*** was identified from plasma samples. Because HSA is the major protein constituent in plasma, the alkylated peptide was easily detected from incubations with both low (3 μM) and high (300 μM) concentrations of **M1**. This observation does not rule out the reaction of **M1** with other minor proteins in plasma. The conjugation of **M1** with HSA in plasma was also shown to be time-dependent (Figure 6). From the dialysis experiments, the alkylation between **M1** and HSA in plasma is confirmed to be irreversible, once a water molecule is lost after the thiol addition, which is consistent with the proposed mechanism (Scheme 3). It is presumed that, until the water molecule is eliminated and the thiol–**M1** adduct becomes "fixed", the reaction is fully reversible. It is possible that HSA may catalyze the dehydration step necessary to generate a stable thiol–**M1** adduct.

The crystal structure of HSA indicates that Cys-34 is on the surface of the protein, with the sulfhydryl group facing inward engaged in a hydrogen bond with Tyr-84 (*10*). However, the sulfhydryl group appears to have access to the aqueous phase and can react with exogenous electrophiles. The oxidation or alkylation of Cys-34 breaks the hydrogen bond to Tyr-84 and induces a conformational change in the protein (*10*). Considering the long half-life of HSA (18 days), irreversible conjugation damage caused by reactive species, such as **M1**, may accumulate. It is known that HSA is responsible for removing endogenous metabolites, such as bilirubin, fatty acids, and bile acids. In addition, structural changes to HSA by the modification of Cys-34 may impair the ability of HSA to function efficiently in detoxification processes. For example, it has been reported that an increased percentage of oxidized Cys-34 in HSA is related to several diseases, including hepatic disease (*20*). HSA irreversible oxidation reduces its ability to transport small molecules and changes its distribution in the body (*21*). In addition, irreversible interaction of reactive metabolite(s) of a drug to HSA simultaneously may have a deleterious effect toward the binding of other drugs because of the limited available binding domains and conformational changes occurring to the protein (*22*). The increased oxidation of Cys-34 decreases the L-Trp (the precursor or serotonin) binding affinity to HSA site II (*23*) and also impairs the HSA binding ability to warfarin and ketoprofen (*24*). Figure 8 shows that the incubation of **M1** with HSA led to a decreased binding affinity toward warfarin. Thus, the loss of HSA function may also lead to the accumulation of these drugs and their metabolites, inducing toxicity.

Figure 7 demonstrates that the increased oxidation of Cys-34 of HSA by *N*,*N*′-diacetyl-L-cystine leads to a diminished ability to conjugate **M1**. It is possible that, in these situations, other proteins can be irreversibly alkylated by **M1** similar to HSA. This in turn may lead to enhanced toxicity mediated by **M1**.

In conclusion, we have demonstrated in *in vitro* studies with human plasma that 2-ABT-*S*-oxide (**M1**) is covalently bound to HSA in an irreversible fashion exclusively at Cys-34. Clearly, the conjugation–dehydration mechanism by which **M1** irreversibly reacts with thiol moieties on HSA and GSH is general, and **M1** has the potential to react with many protein targets. This irreversible alkylation may potentially be responsible for hepatotoxicity of zileuton. Finally, although we have used HSA as a model protein for illustrating the reactivity of **M1**, adducts of HSA may be a useful marker for the formation of reactive intermediates *in vivo*.

Acknowledgment. We thank Molly Zigler Karlinsey and Ran Zhu for their help during the initial phase of the study.

Supporting Information Available: Data for the formation of 2-ABT from HSA and **M1** incubation, **M1** self-condensation in PBS, LC–MS/MS spectra of **M1** dimer and **M1** dimer with water elimination, and LC–MS chromatograms under conditions "a", "b", "c", and "d". This material is available free of charge via the Internet at http://pubs.acs.org.

References

(1) Drazen, J. M., Israel, E., and O'Byrne, P. M. (1999) Treatment of asthma with drugs modifying the leukotriene pathway. *N. Engl. J. Med. 340*, 197–206.
(2) Mansuy, D. (1997) Molecular structure and hepatotoxicity: Compared data about two closely related thiophene compounds. *J. Hepatol. 26* (Suppl. 2), 22–25.
(3) Joshi, E. M., Jeasley, B. H., Chordia, M. D., and Macdonald, T. L. (2004) In vitro metabolism of 2-acetylbenzothiophene: Relevance to zileuton hepatotoxicity. *Chem. Res. Toxicol. 17*, 137–143.
(4) Liebler, C. D., and Guengerich, F. P. (2005) Elucidating mechanisms of drug-induced toxicity. *Nat. Rev. Drug Discovery 4*, 410–420.
(5) Peters, T., Jr. (1996) *All about Albumin: Biochemistry, Genetics, and Medical Applications*, p 431, Acedamic Press, San Diego, CA.
(6) Sudlow, G., Birkett, D. J., and Wade, D. N. (1975) The characterization of two specific drug binding sites on human serum albumin. *Mol. Pharm. 11*, 824–832.
(7) Fasco, M. J., Hauer, C. R., III, Stack, R. F., O'Hehir, C., Barr, J. R., and Eadon, G. A. (2007) Cyanide adducts with human plasma proteins: Albumin as a potential exposure surrogate. *Chem. Res. Toxicol. 20*, 677–684.
(8) Hoffmann, K.-J., Streeter, A. J., Axworthy, D. B., and Baillie, T. A. (1985) Structural characterization of the major covalent adduct formed in vitro between acetaminophen and bovine serum albumin. *Chem.-Biol. Interact. 53*, 155–173.
(9) Talib, J., Beck, J. L., and Ralph, S. F. (2006) A mass spectrometric investigation of the binding of gold antiarthritic agents and the metabolites $[Au(CN)_2]^-$ to human serum albumin. *J. Biol. Inorg. Chem. 11*, 559–570.
(10) Kawakami, A., Kubota, K., Yamada, N., Tagami, U., Takehana, K., Sonaka, I., Suzuki, E., and Hirayama, K. (2006) Identification and characterization of oxidized human serum albumin. *FEBS J. 273*, 3346–3357.
(11) Kwon, C.-H., Maddison, K., LoCastro, L., and Borch, R. F. (1987) Accelerated decomposition of 4-hydroxycyclophosphamide by human serum albumin. *Cancer Res. 47*, 1505–1508.
(12) Pinkerton, T. C., and Koeplinger, K. A. (1990) Determination of warfarin–human serum albumin protein binding parameters by an improved Hummel–Dreyer high-performance liquid chromatographic method using internal surface reversed-phase columns. *Anal. Chem. 62*, 2114–2112.
(13) Kragh-Hansen, U. (1981) Molecular aspects of ligand binding to serum albumin. *Pharmacol. Rev. 33*, 17–53.
(14) Roller, S. G., Dieckhaus, C. M., Santos, W. L., Sofia, R. D., and Macdonald, T. L. (2002) Interaction between human serum albumin and the felbamate metabolites 4-hydroxyl-5-phenyl-[1,3]oxazinan-2-one and 2-phenylpropenal. *Chem. Res. Toxicol. 15*, 815–824.
(15) Ohkawa, T., Norikura, R., and Yoshikawa, T. (2003) Rapid LC–TOFMS method for identification of binding sites of covalent acylglucuronide–albumin complexes. *J. Pharm. Biomed. Anal. 31*, 1167–1176.

(16) Aldini, G., Gamberoni, L., Orioli, M., Beretta, G., Regazzoni, L., Facino, R. M., and Carini, M. (2006) Mass spectrometric characterization of covalent modification of human serum albumin by 4-hydroxyl-trans-2-nonenal. *J. Mass Spectrom. 41*, 1149–1161.

(17) Manoharan, I., and Boopathy, R. (2006) Diisopropylflurophosphate-sensitive aryl acylamidase of fatty acid free human serum albumin. *Arch. Biochem. Biophys. 452*, 186–188.

(18) Valadon, P., Dansette, P. M., Girault, J.-P., Amar, C., and Mansuy, D. (1996) Thiophene sulfoxides as reactive metabolites: Formation upon microsomal oxidation of a 3-aroylthiophene and fate in the presence of nucleophiles in vitro and in vivo. *Chem. Res. Toxicol. 9*, 1403–1413.

(19) Ogasawara, Y., Namai, T., Togawa, T., and Ishii, K. (2006) Formation of albumin dimers induced by exposure to peroxides in human plasma: A possible biomarker for oxidative stress. *Biochem. Biophys. Res. Commun. 340*, 353–358.

(20) Ivanov, A. I., Korolenko, E. A., Korolik, E. V., Firsov, S. P., Zhbankov, R. G., Marchewka, M. K., and Ratajczak, H. (2002) Chronic liver and renal diseases differently affect structure of human serum albumin. *Arch. Biochem. Biophys. 408*, 69–77.

(21) Ivanov, A. I., Korolenko, E. A., Korolik, E. V., Sarnatskaya, V. V., Firsov, S. P., Babushkina, T. A., Zhbankov, R. G., and Nikolaev, V. G. (2006) Dramatic irreversible changes of human serum albumin structure in liver cirrhosis. *New Dev. Liver Cirrhosis Res.* 103–122.

(22) Kargh-Hansen, U., Chuang, U. T. G., and Otagiri, M. (2002) Practical aspects of the ligand-binding and enzymatic properties of human serum albumin. *Biol. Pharm. Bull. 25*, 695–704.

(23) Muscaritoli, M., Peverini, P., Cascino, A., Cangiano, C., Fanfarillo, F., Russo, M., Fava, A., and Rossi, F. F. (1999) Effect of cisplatin and paclitaxel on plasma free tryptophan levels: An in vitro study. *Adv. Exp. Med. Biol. 467*, 275–278.

(24) Mera, K., Anraku, M., Kitamura, K., Nakajou, K., Maruyama, T., and Otagiri, M. (2005) The structure and function of oxidized albumin in hemodialysis patients: Its role in elevated oxidative stress via neutrophil burst. *Biochem. Biophys. Res. Commun. 334*, 1322–1328.

TX7001417